PREDICTIVE MODELLING OF MULTI-PERIOD GEOARCHAEOLOGICAL RESOURCES AT A RIVER CONFLUENCE

Phase II Report (PNUM 3357)

A. G. Brown[1], C. Carey[1], K. Challis[2], A. Howard[3] M. Kincey[2], E. Tetlow[5] & L. Cooper[4]

[1] School of Geography, Archaeology & Earth Resources, Amory Building, Rennes Drive, University of Exeter EX4 4RJ
[2] Institute of Antiquity and Archaeology, University of Birmingham
[3] Birmingham Archaeology & HP Visual & Spatial Technology Centre
[4] University of Leicester Archaeological Services (ULAS)
[5] Birmingham Archaeology Environmental, University of Birmingham

With contributions from P. Toms (University of Gloucester) and D. Hamilton (English Heritage)

February 2007

I Executive summary

This report of Phase II of Predictive Modelling of Multi-period Geoarchaeological Resources at a River Confluence" follows a Phase I report (Brown *et al.* 2005). Phase I has contained the creation of a LiDAR model, geomorphological survey, an archaeological assessment, hand coring, ground penetration radar transects and relative chronostratigraphic modelling. The second phase involved further fieldwork and analyses. The fieldwork included; electrical resistivity survey (ER), ground near infra red (NIR) intensity measurement, mechanical coring and sampling for palaeoecological assessments and dating purposes. The collection of subsurface data by coring was serendipitously augmented by the exposure of several palaeochannels in the La Farge aggregate pit (Warren Farm Quarry) located in the south east of the study area. The analyses included in this report include: ER modelling, analysis of the NIR intensity ground imaging, core analyses, palaeoecological assessments and dating. The palaeoecological assessments included beetles and pollen and the dating included 14C (AMS), dendrochronology and optically stimulated luminescence (OSL).

The ER profiles were run on or close to the GPR and hand coring transects undertaken in Phase I. They showed the normal trade-off between depth and resolution but in general successfully demarcated the channel edges, base and some elements of internal stratigraphy. As suspected ER was not as efficacious as GPR at revealing any intra-gravel stratigraphy and it is suggested that in order to get as full a stratigraphic cross-section as possible across a palaeochannel in gravels both methods should be employed. The ground radar imaging experiments conducted had the aim of trying to quantify and explain variations in LiDAR intensity, which appeared to be systematic (see Phase I).

Mechanical coring with a Geoprobe corer proved to be both efficient and reasonably fast. The collection of samples for OSL also appears to have been successful as none showed signs of post extraction exposure. The stratigraphy of the cores related well to standard analyses including loss on ignition (tom measure organic and carbonate contents) and magnetic susceptibility. Stratigraphic modeling of both borehole/core data and exposure/quarry data using ROCKWORKS is then outlined and approaches to integrating quarry face and borehole data discussed. The analysis of cores (organic content, carbonate content & magnetic susceptibility) suggests that several of the channels had been reoccupied by river flow creating hiatuses in their sedimentary sequences. Pollen and spore samples were processed from a representative selection of cores and the Warren Farm Quarry faces. Concentrations were extremely variable (<1->50,000 grains ml^{-1}) with as expected greater variability in the cores than in the exposures. There was not a consistent relationship with any variables other than a weak and probably partial correlation with pH. Bulk samples recovered directly from the quarry face with a standard volume of 10 litres produced abundant, well-preserved and incredibly diverse beetle assemblages except in the case of a Lateglacial channel. Otherwise preservation was more variable but the role of sample size and the importance of having large quantities (5l – 10l/3 kg), which will provide a representative assemblage, cannot be underestimated.

The dating program showed that the different techniques produced different date frequencies as expected, due to a combination of sampling design and the spatial chronology of the confluence zone. The dendrochronological dates are all clustered around 4.5-4.8 Kyrs BP, whereas the 14C dates ranged from 0.1-7.3 Kyrs BP (excluding the Lateglacial channel) and most fell into the range 1-4.1 Kyrs BP and the OSL dates ranged from 0.9-7.1 Kyrs BP. A definite oral clustering is evident caused by the pattern of channel change and sedimentation.

The chronostratigraphic model constructed in Phase I is then compared with the results of the luminescence (OSL) and radiocarbon dating. Using the stratigraphic, core, dating, LiDAR and geophysical data an evolutionary /diachronic geoarchaeological model of t he Trent-Soar confluence zone is proposed. Thi s model pl aces heavy emphasis o n a vulsion, t he r e-occupation of channels and lev ee and overba nk sedi mentation as th e ke y processes t hat pattern the geoa rchaeological record and no t meander migration, late ral er osion and aggradation th at ar e normally s een as the patterning processes. This h as i mportant implications for si milar high-en ergy floodplains as well as the lower sedi mentary fills of lowland flo odplains, in that it constrains and patte rns t he distribu tion of arc haeological artefact and s tructure s urvival. The report concludes w ith the main con clusions of the techniques used in Phase II an d prese nts new researc h d irections and p resents a methodological state ment for geo archaeological survey s of si milar floo dplain confluence zones.

II Acknowledgements

This report has been written with the considerable support and help from many individuals. Technical and cartographic advice is acknowledged from S. Rouillard, H. Jones and D. Fraser. The landowners of the target area must be thanked for access and in particular Lafarge Aggregates Ltd. for both access and the provision of data. The project is als o grateful t o st aff of th e HP Visualization Centre at Birmingham University and U niversity of Leicest er Archaeol ogical Serv ices. English He ritage is acknowledged as the funding body through the ALSF.

III Report Contents
I. Executive Summary
II. Acknowledgements
III. Contents
IV. List of figures
V. List of tables

III Contents

Chapter 1: Introduction
1.1 Introduction to the study
1.2 Summary of objectives
1.3 The study area
1.4 Project background
1.5 Previous work

Chapter 2: Archaeological Assessment of the Study Area and its Environs
2.1 Lower-Middle Palaeolithic
2.2 Upper Palaeolithic
2.3 Mesolithic
2.4 Neolithic – Mid Bronze Age
2.5 Late Bronze Age – Iron Age
2.6 Romano-British
2.7 Anglo-Saxon
2.8 Medieval
2.9 Post-medieval
2.10 Geomorphology and the archaeological resource
2.11 Conclusions

Chapter 3: Materials and methods
3.1 OSL sampling
3.1.1 Optical dating: Mechanisms and principles
3.1.2 Sample Collection and Preparation
3.1.3 Acquisition and accuracy of D_e value
3.1.4 Laboratory Factors
3.1.4.1 Feldspar contamination
3.1.4.2 Preheating
3.4.1.3 Irradiation
3.1.4.3 Internal consistency
3.1.5 Environmental factors
3.1.5.1 Incomplete zeroing
3.1.5.2 Turbation
3.1.6 Acquisition and accuracy of D_r value
3.1.7 Estimation of Age

3.1.8 Analytical uncertainty
3.1.9 Intrinsic Assessment of Reliability
3.2 Radiocarbon and pollen sample collection
3.2.1 Tin collection Warren Farm Quarry
3.2.2 Gouge core sampling
3.2.3 Pollen sample methods
3.2.4 Radiocarbon sample methods
3.2.4.1 Sampling
3.2.4.2 Macrofossils
3.2.4.3 Sediment
3.3 Dendrochronological dating
3.4 Core stratigraphy, physical and chemical parameters
3.4.1 Organic content
3.4.2 Carbonate content
3.4.3 Magnetic susceptibility
3.4.4 Eh
3.4.5 pH
3.4.6 Geochemistry
3.4.7 Grain size
3.4.8 Tin/core sediment stratigraphy
3.4.9 Data ordering and analysis methods
3.5 Pollen and Spore Assessment
3.6 Coleopteran Assessment
3.6.1 Processing and Identification
3.6.1.1 Processing – The Paraffin Flotation Technique
3.6.1.1 Sorting and Identification
3.6.2 The objective ana lysis, quantification an d presen tation of p alaeoentomology as an environmental indicator
3.6.3 Difficulties with environmental interpretation using palaeoentomology
3.6.4 A solution to problems of interpretation
3.6.5 Visual Presentation of Data
3.7 Field survey
3.7.1 Section recording
3.7.2 Field survey
3.8 Electrical resistivity (ER) materials and methods
3.8.1 Geoprospection within alluvial environments
3.8.2 GPR prospection within alluvial environments – a resume
3.8.3 ER prospection within alluvial environments
3.8.4 An introduction to ER survey
3.8.3.1 Electrical resisitivity and sediment stratigraphy
3.8.4 ER materials and methods
3.8.4.1 Instrumentation and data collection parameters
3.8.4.2 Field methodology
3.8.4.3 Data download and pseudosection viewing
3.8.4.4 Data inversion
3.8.4.5 Data interpretation
3.8.6 The aims of ER survey within this study
3.9 Standardised keys for stratigraphy descriptions
3.10 LiDAR intensity ground scanning
3.10.1 Introduction

3.10.2 Aims and Objectives
3.10.3 Method Statement
3.10.3.1 Toposil Moisture and Intensity: Broad Area Survey
3.10.3.2 Topsoil Moisture, Organic Content and Intensity: Detailed Study
3.11 Data archive and query
3.12 Ground penetrating radar materials and methods

Chapter 4: stratigraphic modelling
4.1 Stratigraphic overview of the study area
4.1.1 Introduction to the study area
4.1.1.1 Geology
4.1.1.2 Topography
4.1.1.3 Stratigraphy
4.1.1.4 Terrace 2 (Devensian) stratigraphy
4.1.1.5 Terrace 1 (Holocene) stratigraphy
4.1.1.6 Modern floodplain stratigraphy
4.2 Three-dimensional stratigraphic modelling of the study area using existing data sets
4.2.1 Outline
4.2.2 Methodology of wider area 3D stratigraphic model
4.3.3 Summary of modelling

Chapter 5: Chronostratigraphy
5.1 Original chronostratigraphic model
5.2 RC dating of palaeochannels
5.3 OSL dating of intervening valley floor
5.4 Dendrochronological dating of trees
5.5 Summary

Chapter 6: Palaeoenvironmental analysis and taphonomy
6.1 Palaeoenvironmental sample stratigraphy
6.1.1 Core MFC2
6.1.2. Core T1C7
6.1.3 Core T1C10
6.1.4 Core T1C12
6.1.5 Core T1C14
6.1.6 Core TFGC14
6.1.7 WQFC1
6.1.8 WQFC2
6.1.9 WQFC3
6.10 WQFC5
6.11 Comparison of palaeoenvironmental samples organic contents
6.2 Coleopteran analysis
6.2.1 Preservation
6.2.2 Coleopteran analysis: palaeoecology
6.2.3 Discussion
6.1.4 Palaeochannel Relationships

6.1.5 Conclusions
6.2 Pollen and Spore Assessment
6.3 Map of palaeoenvironmental potential over the study area
6.4 Summary

Chapter 7: Investigating backscattered intensity of Airborne LiDAR
7.1 Toposil Moisture and Intensity: Broad Area Survey
7.1.1 Discussion
7.2 Topsoil Moisture, Organic Content and Intensity: Detailed Study
7.2.1 AREA FF
7.2.2 AREA MTF
7.2.3 AREA MF
7.3 Conclusions

Chapter 8: Electrical resistivity survey
8.3 Terrace 2 ER surveys
8.3.1.1 Transect T2A
8.4 Terrace 1 ER surveys
8.4.1 Transect T1A
8.4.2 Transect T1B
8.4.3 Transect T1C and T1D: comparison of electrode spacing
8.4.3.1 Transect T1C
8.4.3.2 Transect T1D
8.4.3.3 A comparison between ER transects T1C and T1D
8.4.4 Transect T1E
8.4.5 ER transect T1F
8.4.6 ER transect T1G
8.4.7 ER transect T1H
8.4.8 *ER transect T1J*
8.4.9 ER transect T1K
8.5 Modern Floodplain ER surveys
8.5.1 ER Transect MFA 1m electrode spacing
8.5.2 ER transect MFB 0.5m electrode spacing
8.5.3 Comparing 1m and 0.5m electrode spacing on the Modern Floodplain
8.6 Methodological considerations of using ER
8.6.1 Relationship of ER data to electrode spacing
8.6.2 Relationship of ER data to stratigraphy
8.6.3 Relationship of ER data to GPR data
8.7 Ranking palaeochannels by biotaphonomic potential based on ER resistivity values
8.8 Overview and summary

Chapter 9. A geoarchaeological model of the Trent-Soar Confluence Zone
9.1 Generalising and modelling the chronostratigraphy
9.2 Development of a valley floor evolution model

Chapter 10. Conclusions and methodological Implications

10.1 Conclusions
10.2 New research directions
10.3 Methodological Statement for Archaeological Prospection in Confluence Zones

11 Bibliography

12 Appendices

Appendix A. ^{14}C report (Dr. Hamilton)
Appendix B. OSL Report (Dr. P. Toms)
Appendix C. Dendrochronology (Dr. R Howard)

IV. List of figures.

Chapter 1

Fig 1.1. The location of the study area.

Chapter 2

Fig 2.1: The study area mapped by geological stage.
Fig 2.2: The archaeological resource plotted by its method of investigation, against the LiDAR last pulse DTM.
Fig 2.3: The archaeological resource plotted by period.
Fig 2.4: The 'Lockington Villa' complex within the study area.
Fig 2.5: The cropmark enclosure on terrace 1.

Chapter 3

Fig 3.1: The Geoprobe coring rig, about to commence a drive.
Fig 3.2: A sample recovered from the Geoprobe.
Fig 3.3: The locations of the palaeoenvironmental samples.
Fig 3.4: The location of the palaeochannels sampled in the quarry and the exposed section that were drawn.
Fig 3.5: Sections 1 and 2 WFQ.
Fig 3.6: Sections 3 and 4 WFQ.
Fig 3.7: Palaeochannel WFQ C1 during sampling.
Fig 3.7: Palaeochannel WFQ C2 during sampling, with the tins *in-situ* before removal.
Fig 3.8: Palaeochannel WQFC3.
Fig 3.9: The basis of a resistivity measurement.
Fig 3.10: The Wenner and Schlumberger arrays.
Fig 3.11: The data collection points on the 0.5m electrode spacing first transect.
Fig 3.12: The data collection points on the 0.5m second and subsequent transects.
Fig 3.13: The data collection points on the 1m electrode spacing first transect.
Fig 3.14: The data collection points on the 1m electrode spacing second and subsequent transects.
Fig 3.15: The data collection points on the 1m electrode spacing first transect.
Fig 3.16: ER transect running across a palaeochannel on the lower floodplain.
Fig 3.17: Recording the position of the ER transect T1F using dGPS.
Fig 3.18: Modified Troel Smith key for sediment descriptions.
Fig 3.19: Air-photographic, LiDAR elevation and LiDAR intensity data for a part of the Hemington Terrace unit at Lockington.
Fig 3.20: LiDAR elevation (bottom) and Intensity (Top) data for the Lockington study area.
Fig 3.21: Graph showing the measured reflectance of sediments of differing moisture organic content and particle size across the spectrum.
Fig 3.22: Sample locations for soil moisture/intensity comparison.
Fig 3.23: Lockington study area. LiDAR LPG elevation data with detailed LiDAR intensity study areas highlighted in red.
Fig 3.24: Lockington. Field collection of volumetric soil moisture data at regular grid intervals using a Delta T Devices Theta Probe.
Fig 3.25: Lockington. Field collection sediment samples for organic content analysis.

Chapter 4

Fig 4.1: Location of data points for the 3D stratigraphic modelling (map by permission of OS).
Fig 4.2: Location of stratigraphic fence diagrams (map by permission of OS).
Fig 4.3: ArcScene visualisation of study area stratigraphic fence diagrams below lidar elevation model.
Fig 4.4: ArcScene visualisation of Terrace 1 stratigraphic fence diagrams below lidar elevation model.
Fig 4.5: Interpolated surface showing base of alluvium across the study area (map by permission of OS).
Fig 4.6: Location of Warren Farm Quarry and the active extraction area (map by permission of OS).

Chapter 5

Fig 5.1: The ^{14}C dates plotted at core/sample locations.

Fig 5.2: A plot of the cores with basal dates against surface height OD.
Fig 5.3: The OSL dates plotted at sample locations.
Fig 5.4: The OSL dates plotted by height.
Fig 5.5: Photograph of the tree trunks from Warrens Farm Quarry that were dendrochronologically dated.

Chapter 6

Fig 6.1: The location of the palaeoenvironmental samples and their basal dates ascertained through radiocarbon dating.
Fig 6.2: Core MFC2 stratigraphy shown against organic content, carbonate content and magnetic susceptibility.
Fig 6.3: Core MFC2 stratigraphy with pollen sample points and radiocarbon dates.
Fig 6.4: Core T1C7 stratigraphy shown against organic content, carbonate content and magnetic susceptibility.
Fig 6.5: Core T1C7 stratigraphy with pollen sample points and radiocarbon dates.
Fig 6.6: Core T1C10 stratigraphy shown against organic content, carbonate content and magnetic susceptibility.
Fig 6.7: Core T1C7 stratigraphy with pollen sample points and radiocarbon dates.
Fig 6.8: Core T1C12 stratigraphy shown against organic content, carbonate content and magnetic susceptibility.
Fig 6.9: Core T1C12 stratigraphy with pollen sample points and radiocarbon dates.
Fig 6.10: Core T1C14 stratigraphy shown against organic content, carbonate content and magnetic susceptibility.
Fig 6.11: Core T1C14 stratigraphy with pollen sample points and radiocarbon dates.
Fig 6.12: Core TFGC14 stratigraphy shown against organic content, carbonate content and magnetic susceptibility.
Fig 6.13: Core TFGC14 stratigraphy with pollen sample points and radiocarbon dates.
Fig 6.14: Core WQFC1 stratigraphy shown against organic content, carbonate content, magnetic susceptibility Eh and Ph.
Fig 6.15: WQFC1 stratigraphy with pollen sample points and radiocarbon dates.
Fig 6.16: WQFC2 stratigraphy shown against organic content, carbonate content, magnetic susceptibility Eh and pH.
Fig 6.17: WQFC2 stratigraphy with pollen sample points and radiocarbon dates.
Fig 6.18: WQFC3 stratigraphy shown against organic content, carbonate content, magnetic susceptibility Eh and pH.
Fig 6.19: WQFC3 stratigraphy with pollen sample points and radiocarbon dates.
Fig 6.20: WQFC5 stratigraphy shown against organic content, carbonate content, magnetic susceptibility Eh and pH.
Fig 6.21: WQFC5 stratigraphy with pollen sample points and radiocarbon dates.
Fig 6.22: The palaeoenvironmental samples shown by mean organic content.
Fig 6.23: Warren Farm Quarry species ecological groups.
Fig 6.24: Variation of % damaged (grains) with depth all data.
Fig 6.25: Variation of % damaged (grains) with depth cores only.
Fig 6.26: Mean concentration of pollen and spores against mean core pH.

Chapter 7

Fig 7.1: Lockington study area. LiDAR LPG elevation data with detailed LiDAR intensity study areas highlighted in red.
Fig 7.2: Scatter plot of LiDAR intensity and volumetric soil moisture for study area.
Fig 7.3: Scatter plot of LiDAR intensity and volumetric soil moisture for Hemington Terrace only.
Fig 7.4: Scatter plot of LiDAR intensity and volumetric soil moisture for alluvium only.
Fig 7.5: Lockington, selected sample locations.
Fig 7.6: Scatter plot of LiDAR intensity and volumetric soil moisture for selected area.
Fig 7.7: Lockington study area FF.
Fig. 7.8: Lockington area FF showing left airborne LiDAR DSM and right airborne LiDAR intensity.
Fig 7.9: Lockington area FF showing left topsoil organic content and right volumetric soil moisture of topsoil.
Fig 7.10: Lockington area FF showing topsoil organic content.
Fig 7.11: Lockington area FF scatter plot showing topsoil organic content and LiDAR intensity.
Fig 7.12: Lockington area FF showing topsoil volumetric soil moisture.
Fig 7.13: Lockington area FF scatter plot showing topsoil volumetric soil moisture and LiDAR intensity.
Fig 7.14: Lockington, FF study area - Volumetric soil moisture and statistics.
Fig 7.15: Lockington, FF study area - Topsoil organic content and statistics.
Fig 7.16: Lockington area MTF: Left, LiDAR elevation data and right LiDAR intensity values.

Fig 7.17: Lockington area MTF: Left, LiDAR intensity values and right intensity with interpolated volumetric soil moisture for each study area superimposed.
Fig 7.18: Lockington area MTF1: Scatter plot of LiDAR intensity and volumetric soil moisture.
Fig 7.19: Lockington area MTF2: Scatter plot of LiDAR intensity and volumetric soil moisture.
Fig 7.20: Lockington MTF1 study area - Volumetric soil moisture statistics.
Fig 7.21: Lockington, MTF2 study area - Volumetric soil moisture (%) statistics.
Fig 7.22: Lockington study area MF showing channel (left) and bar feature (right).
Fig 7.23: Lockington study area MF LiDAR elevation (left) and intensity (right).
Fig 7.24: Lockington study area MF volumetric soil moisture (left) and topsoil organic content (right).
Fig 7.25: Lockington study area MF topsoil organic content.
Fig 7.26: Lockington study area MF scatter plot of LiDAR intensity and topsoil organic content.
Fig 7.27: Lockington study area MF volumetric soil.
Fig 7.28: Lockington study area MF scatter plot of LiDAR intensity and volumetric soil.
Fig 7.29: Lockinton, MF study area - Volumetric soil moisture statistics.
Fig 7.30: Lockington, MF study area - Topsoil organic content.

Chapter 8

Fig 8.1: The location of T2A on the upper Devensian Holme Pierrepont terrace 2.
Fig 8.2: Transect T2A ER section.
Fig 8.3: The location of transects T1A and T1B, at the junction between terrace 2 and terrace 1.
Fig 8.4: The stratigraphy of transects T1A and T1B.
Fig 8.5: ER transect T1A.
Fig 8.6: ER transect T1B. The palaeochannel in the section is an obvious feature.
Fig 8.7: The location of ER transects T1C and T1D.
Fig 8.8: The ER transect T1C.
Fig 8.9: The ER transect T1D.
Fig 8.10: The location of ER transect T1E, placed on the LiDAR LP DTM.
Fig 8.11: ER transect T1E placed on the LiDAR intensity survey.
Fig 8.12: Earth resistance survey over the same area as T1E.
Fig 8.13: ER transect T1E.
Fig 8.14: Photograph of ER transect T1F
Fig 8.15: Location of the ER transect T1F.
Fig 8.16: ER transect T1F.
Fig 8.17: Location of ER transect T1G.
Fig 8.18: The ER transect T1G.
Fig 8.19: Location of transect T1H on terrace 1.
Fig 8.20: ER transect T1H.
Fig 8.21: The location of transect T1J.
Fig 8.22: The ER transect T1J, gouge core stratigraphy combined with GPR and ER sections.
Fig 8.23: The ER transect T1J with interpretation.
Fig 8.24: Location of ER transect T1K, on the same transect line as T1A.
Fig 8.25: ER transect T1K, raw data (top) and with gouge core stratigraphy (bottom).
Fig 8.26: ER section T1K with interpretation.
Fig 8.27: Comparison of the ER sections T1K and T1A, comparing the 2m and 1m electrode spacings.
Fig 8.28: The location of transects MFA and MFB.
Fig 8.29: ER transect MFA.
Fig 8.30: ER transect MFB.
Fig 8.31: Combined visualisation of GPR and ER data, with the ER section at 80% transparency.
Fig 8.32: Combined visualisation of GPR and ER data, with the ER section at 60% transparency.
Fig 8.33: Combined visualisation of GPR and ER data, with the ER section at 40% transparency.
Fig 8.34: Combined visualisation of GPR and ER data, with the ER section at 20% transparency.

Chapter 9

Fig 9.1: Re-zoned study area using basal radiocarbon and OSL dates (left) and chronostratigraphic model (right).
Fig 9.2: The chronostratigraphic model with OSL dates shown.
Fig 9.3: The chronostratigraphic model with OSL dates shown.
Fig 9.4: Neolithic channels flowing approximately S-N and depositing terrace 1.
Fig 9.5: Bronze Age channels trending SE-NW abandoned on terrace 1.

Fig 9.6: Iron-Age-early Post Roman. Note older Neolithic – Bronze Age core within meander loop.
Fig 9.7: New Soar channel location Romano-British – Medieval.
Fig 9.8: Medieval-early Historic abandonment of loop and channel shift to the NE.
Fig 9.9: Post Medieval northward migration of Trent channel and establishment of the present junction.

V. List of tables

Chapter 3

Tab 3.1: Sites used for environmental sampling with number of pollen samples taken for assessment.
Tab 3.2: Species ecological groups.
Tab 3.3: General resistivity and conductivity values of some rocks and soils.
Tab 3.4: Table of predicted resistivity ranking of sediment units within the study area, on a *pre-hoc* basis before survey.
Tab 3.5: ER surveys undertaken.

Chapter 5

Tab 5.1: Details of samples from Lockington Quarry on the river Trent in Leicestershire.
Tab 5.2: Results of the cross-matching of site chronology LOKQSQ01 and relevant reference chronologies when first ring date is 2928 BC and last ring date is 2629 BC.
Tab 5.3: Results of the cross-matching of sample LOK-Q06 and relevant reference chronologies when first ring date is 2623 BC and last ring date is 22519 BC.

Chapter 6

Tab 6.1: Preservation of insect sclera from the Warrens Farm Quarry cores.
Tab 6.2: Pollen and spore concentrations and descriptive classes.
Tab 6.3: Summary statistics for pollen and spore assessment.
Tab 6.4: Correlation matrix for sediment, pollen and environmental variables.
Tab 6.5: Correlation matrix for sediment, pollen and environmental variables, core samples only.
Tab 6.6: Mean values for pollen taphanomic variables against mean core pH and Eh.
Tab 6.7: Ranks of the palaeoenvironmental (pollen and spore) potential of the cores.

Chapter 8

Tab 8.1: Summary of field considerations of using different electrode spacings.
Tab 8.2: Summary of the data capture properties of different electrode intervals.
Tab 8.3: Ranking of biotaphonomic potential of palaeochannels based on resistivity values.

Chapter 9

Tab. 9.1: Correspondance (confusion) of matrix of chronostratigraphic model with observed dates.

Chapter 1: Introduction

1.1 Introduction to the study

This project has been framed to address the core ALSF theme of developing capacity to manage aggregate extraction landscapes in the future (English Heritage 2004). In addition it addresses several objective two ALSF themes, namely:

1) Characterising the [archaeological] resource and developing evaluation frameworks, predictive tools and mitigation strategies.

2) Development [of] remote sensing and predictive techniques and mitigation strategies.

3) Training and professional development and to raise awareness of issues and to improve the quality of historic environment work undertaken in response to aggregate extraction.

4) Development of advanced visualisation and immersive three-dimensional models of landscape development, largely part of phase 2 of the project, has the potential to address the theme of interpretation and outreach to the community of the knowledge gained from work related to aggregate extraction.

1.2 Summary of objectives

The full detail of objectives are given in the original Project Design (PNUM3357, phase II PD). The principal aim of this project is to predictively model the landscape of a major river confluence over a time-scale of millennia and at a spatial scale appropriate for archaeological management. The overall purpose is:

1) To establish a rigorous research model for the future development of predetermination designs for site evaluation.
2) To assess the effectiveness of various airborne and ground based remote sensing methods in alluvial environments.
3) To derive relationships between pre-extraction site survey data and likely chronostratigraphic and environmental data as part of archaeological assessment.

This research will assist regulatory bodies (i.e. County Councils) in demanding and specifying rapid evaluations of geoarchaeological potential as part of the implementation of PPG16. The novelty of the approach lies in the integration of high-resolution topographical, archaeological and geological (three-dimensional sub-surface) data within a Geographical Information System (GIS). The technical innovation will be the combination of Inteferometric Synthetic Aperture Radar (IFSAR), Airborne Laser Altimetry (LiDAR), CW Differential GPS (DGPS), Ground Penetrating Radar (GPR) and other ground based remote sensing techniques. This research will contribute to the framework for management of the archaeological resource in the Trent Valley developed through Trent Valley GeoArchaeology (Bishop *et al.* 2002) and provide a transferable model for the geoarchaeological investigation and management of valley floor archaeology.

1.3 The study area

The study area is a block of the Trent/Soar confluence landscape approximately 2 by 4 km (Fig. 1.1; East Midlands, U.K). The area abuts the main area of Trent Valley GeoArchaeology (TVG) interest and is close to but not overlapping sites of continuing research by University of Leicester Archaeological Services (ULAS). The area is not zoned for aggregate extraction although the area to the west is.

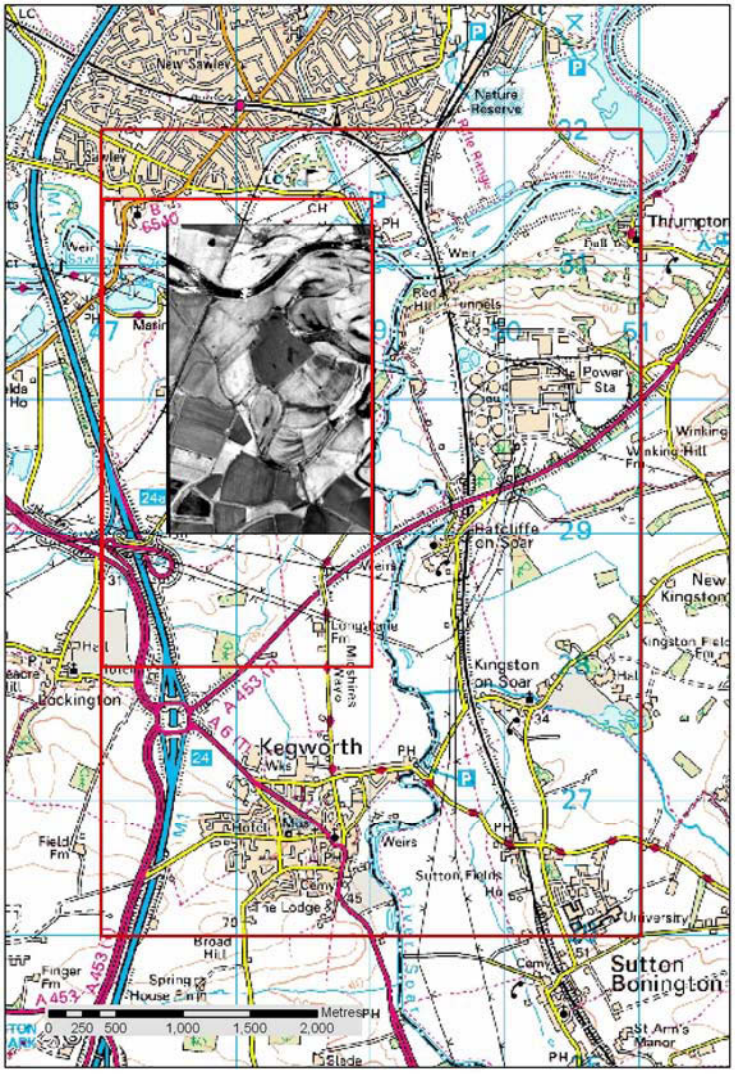

Fig 1.1: The study area over the 1:50,000 Ordnance Survey map (by permission of OS).

1.4 Project background

Recent archaeological work on the Thames and other British floodplains suggests that river confluences have been the foci of settlement and human activity since the earliest post-glacial periods. At confluences the high density of palaeochannels provides an opportunity to determine records of past environmental change. Migration of rivers channels also provides an environment with high potential for the burial and preservation *in situ* of cultural and environmental materials. Unfortunately this potential is generally only realised during the destruction of the land surface by development and subsequent 'rescue' archaeological investigation. It is the nature of the archaeological record of floodplains that there is a direct link between the geomorphology, including the nature and distribution of channels, levees, gravel bars, terrace remnants, etc. and the distribution and nature of archaeological materials, from flint scatters to structures. Therefore there is a predictive capability in the subsurface geomorphology, stratigraphy and buried land surfaces.

1.5 Previous work

The Middle Trent is one of the archaeologically richest stretches of alluvial landscape in the UK. Finds include medieval bridges (the Hemington Bridges excavations, funded by English Heritage), a Norman milldam, fishweirs and dugout canoes (Salisbury *et al*., 1984; Cooper, 2003). The study area (a block of floodplain 8 km^2) is centred on the Lockington Marshes at the confluence of the Trent and Soar. This area is rich in cultural archaeology lying immediately east of the nationally significant prehistoric ritual landscape of the Derbyshire Trent Valley (Riley, 1987). Recent finds from a Bronze Age barrow cemetery (Hughes, 2000) strongly suggests that this prehistoric ritual landscape extends into the area. In the Romano-British period the area lies in the hinterland of a villa complex at Lockington and a small town, possibly a centre of ritual/religion at Red Hill, Ratcliffe on Soar (Elsdon, 1982). The area, although not threatened with imminent destruction, is earmarked for longer-term development. Pilot studies indicate the high buried archaeological potential of the locality (Ripper, 1997), which combined with a high density of sites suitable for palaeoenvironmental studies (Howard, 1997) provide an ideal zone for detailed modelling. Work by Trent Valley GeoArchaeology (Knight and Howard, 2004) has done much to provide a regional framework for the cultural, landscape and environmental archaeology of the Trent Valley. The present proposal provides an opportunity to build constructively on that framework through detailed consideration of a significant confluence zone, targeted fieldwork and innovative use of GIS and allied technologies.